Cellular BioMEMS

Academic and Research Staff
Professor Joel Voldman

Postdoctoral Associates
Katarina Blagović, Yi-Chin Toh, Wei Mong Tsang

Graduate Students
Salil Desai, Joseph Kovac, Melanie Hoehl, Nick Mittal, Laralynne Przybyla, Somponnat Sampattavanich, Brian Taff, Michael Vahey

Undergraduate Students
Ylaine Gerardin, Spencer Murray

Technical and Support Staff
Chadwick Collins

Laboratory for Cellular BioMEMS – Research Themes

Our group performs research on BioMEMS, applying microfabrication technology to illuminate biological systems, especially at the cellular level. Specifically, we develop technologies that are used to manipulate cells or make measurements from them. Our research builds upon various disciplines: electrical engineering, microfabrication, bioengineering, surface science, fluid mechanics, mass transport, etc. We take a quantitative approach to designing our technology, using both analytical and numerical modeling to gain fundamental understanding of the technologies that we create. We then take our designs through microfabrication to packaging and testing and to biological assay. Our applications have a strong emphasis on stem cell biology and cell sorting.

1. Optical cell sorting for cell cytometry

Sponsors
NDSEG graduate fellowship, NSF graduate fellowship, NIH NCRR, Singapore-MIT Alliance

Project Staff
Ylaine Gerardin
Joseph Kovac

Overview

The goal of this research is to develop new technologies that enable image-based sorting of mammalian cells. Fluorescence-activated cell sorting (FACS) is the most widespread cell-sorting technology, but FACS is unable to resolve sub-cellular or time-varying fluorescence. This limitation prevents researchers from isolating cells based on information such as spatial and/or temporal protein expression and general morphology. This limitation strongly constrains the types of pooled genetic screens that can be performed and greatly increases the amount of effort required to isolate clones of a particular phenotype that requires imaging to recognize. To address this limitation, we have developed an inexpensive, user-friendly sorting method that augments a standard automated fluorescence microscope with the ability to sort cells based on images. Because of the low cost, user friendliness, and easy integration of our method into existing microscopes, our approach will enable fundamentally new biological assays and shorten or eliminate commonplace tedious practices.

Technology Background

This effort has utilized microfabricated/microfluidic approaches to cell sorting, including purely dielectrophoretic (DEP) trap arrays, passive hydrodynamic trap arrays with active DEP-based cell release, and passive microwell arrays with optical cell release to permit sorting of non-adhered cells. As these proceeding technologies were best suited to operate with non-adherent cells, we have recently turned our focus to developing a solution for adherent cells. Our approach to sorting adherent cells uses a photolithography-inspired method without the use of microfluidics (Figure 1). We first plate adherent cells into a dish and identify cells of interest using a microscope, noting the locations of desired cells within the dish relative to alignment marks. A computer program interprets the alignment mark and cell locations and generates a mask image, with black features corresponding to locations of desired cells. We then print the mask image to a transparency using a standard inkjet printer. After aligning the transparency mask to the back of the cell culture dish, opaque mask features reside beneath desired cells.

We then mix a prepolymer solution consisting of cell culture media, a UV-photoinitiator, and poly(ethylene glycol) diacrylate (PEGDA) monomer. We add the prepolymer to the cell culture dish and shine ultraviolet (UV) light from a standard fluorescence microscope fluorescence source through the transparency and into the dish. The prepolymer then crosslinks into a hydrogel in all unmasked locations, encapsulating undesired cells. The desired cells, which are not encapsulated, can be enzymatically released from the substrate and recovered. The overall technique requires standard equipment found in biology labs and inexpensive reagents (<$10 per experiment), encouraging widespread adoption.

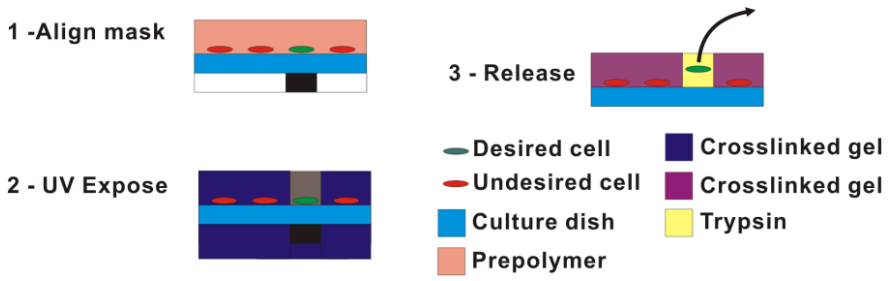

Figure 1. Schematic of sorting method. 1) Mask is aligned such that opaque features reside behind desired cells; prepolymer is added. 2) UV light crosslinks polymer in exposed regions, encapsulating undesired cells. 3) Un-encapsulated desired cells are released and reclaimed.

Current Research

We are focused both on characterization and application of our technique. As sort purity varies inversely with the smallest well that can be patterned into the gel, we have examined the release efficiency of cells from wells of various diameters; presently we have achieved robust release from well sizes down to 500 μm in diameter (Figure 2). We are also characterizing mask printing reliability and resolution and our ability to align the masks by hand, all of which factor into the purity of sorted populations. Furthermore, we have

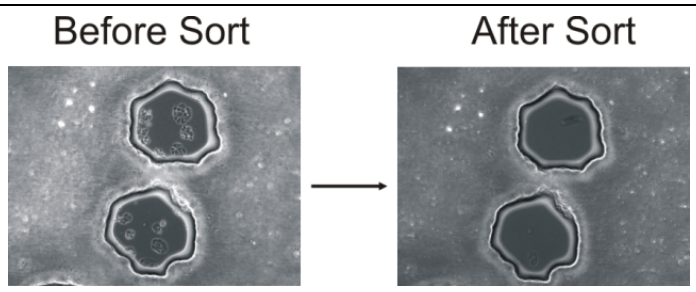

Figure 2. Image showing a 500-μm-diameter well surrounding desired MCF7 cells before and after sorting; cells in wells are released while cells within hydrogel remain.

investigated the effect that the prepolymer blend has with respect to cell health and minimum spot size.

We have directly demonstrated viable cell sorting and enrichment of a target, minority population (Figure 3). In these experiments, we have shown the method's ability to viably isolate desired cells from a background population of undesired cells with up to 100% output purity. We intend to further characterize the variation of purity and throughput with initial cell plating density and incidence rate of the minority cell population. Finally, we intend to demonstrate selection of image-based phenotypes in a biological application demonstrating the class of assays that our method will enable in an inexpensive, user friendly manner adoptable by many biology labs.

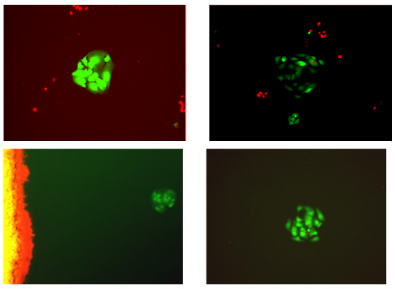

Figure 3: Images of a mixed population of red-fluorescent (majority, undesired) cells and green-fluorescent (minority, desired) cells before (top row) and after (bottom row) sorting.

2. Microsystems and Cell Health

Sponsors
NIH NCRR
Singapore-MIT Alliance

Project Staff
Salil Desai

Overview

Microsystems are increasingly used in the manipulation, patterning and sorting of cells. Critical to the widespread adoption of these new technologies is development of an understanding of their impact on cellular physiology. Here we provide results obtained from a microsystem platform capable of applying one commonly used microscale stimulus, namely electric fields, and subsequently assaying cell physiological state using sensitive cell-based sensors coupled with quantitative fluorescence microscopy. This electric field-based microsystem enables the screening of electrical waveforms to 16 independently addressable culture sites, each capable of electrically stimulating ~1000 cells. Independent control of electrical waveforms enabled performing screens across electric field strength, frequency, and application duration.

Technology Background and Results

The microsystem consists of a chip with 16 individually addressable arrayed electrodes and support electronics to generate the desired waveforms. Cell-based sensors are seeded on the chip and then the entire assembly is clamped and placed in a standard cell culture incubator, where a computer-controlled, custom-designed switch box automatically and autonomously applies arbitrary stimulation waveforms (varying voltage, frequency, and duration) to individual electrode sites.

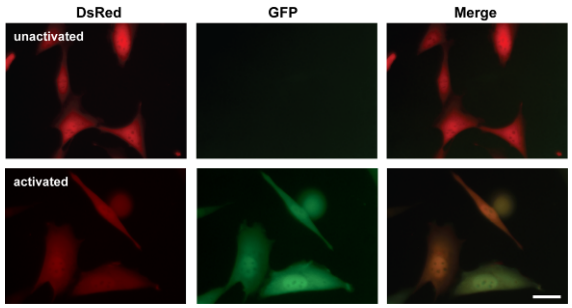

Figure 4: Cell-based sensor. Fluorescence microscopy images of cells before (top panel) and after (bottom panel) stress-based activation. Images show constitutive DsRed expression (left column) and inducible EGFP expression (middle column). Scale bar 25 μm.

Our cell-based sensor consists of specifically engineered a reporter cell line that monitors the cells' general stress response pathway

(Figure 4). This reporter cell line expresses green fluorescent protein (GFP) under the control of a heat shock element (HSE) promoter construct. The HSE promoter regulates the stress response under thermal, chemical, and other environmental stresses. The reporter shows a 10× increase in GFP fluorescence in response to stress, providing a high signal-to-noise ratio for the detection of stressed states.

One set of experiments investigated how stress activation varied across frequency (Figure 5). The frequency sweep shows slight increase (~20%) in activation from 50 MHz down to 1 MHz, and then a steeper increase (~25%) from 1 MHz down to 250 kHz. This general trend of relatively flat high-frequency response and a sharp increase at low frequencies repeated itself at different activation voltages. Electric fields are known to generate reactive oxygen species at the electrode-electrolyte interface, which are generally known to stress cells. To investigate whether reactive oxygen species played a role in the observed variations of stress with frequency, we added an oxygen scavenger, catalase, to our stress reporter cells and observed a significant decrease in reporter activation, confirming the central role of ROS in the frequency-dependent stress activation (Figure 6).

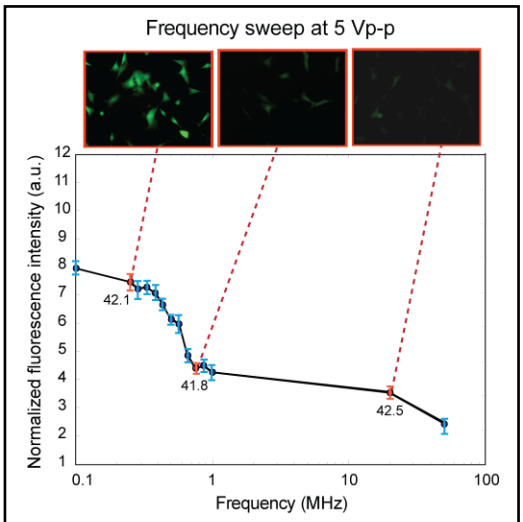

Figure 5: Frequency sweep. Stress induction across frequency (100 kHz through 50 MHz showing increased stress at lower frequencies. Top panel shows representative images across three points in frequency.

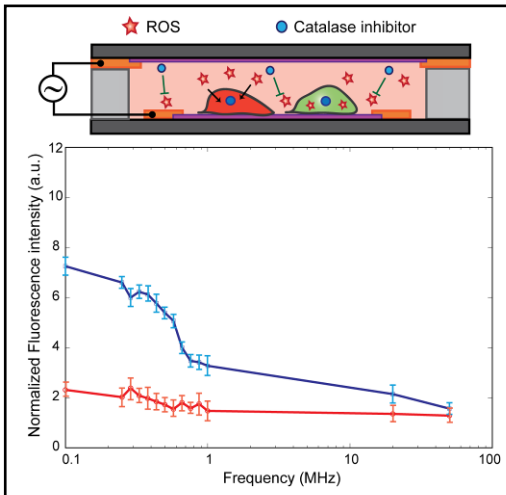

Figure 6: Role of ROS. Frequency sweep with characteristic high-stress at low frequency (blue line) is greatly attenuated with addition of the reactive oxygen radical scavenger, catalase (red line), indicating that ROS is a dominant contributor to stress at low frequencies.

Current Research

To demonstrate the full power of cell-based sensors for measuring the physiological impact of microsystems, a larger set of parental cell lines would need to be used to construct reporters. This would provide end-users with at the very least a cell line with similar morphology and lineage to their cell line of interest. While it would be prohibitively time consuming to generate large libraries of such sensors, the replication of sensors in at least 4-5 other lineages would decrease their barrier to entry. As a first step toward this, we have constructed a stress reporter cell line in nonadherent BA/F3 pro B cells (Figure 7). In particular, the construction of this cell line could prove synergistic with efforts to build a system for screening electric-field effects in non-adherent cells.

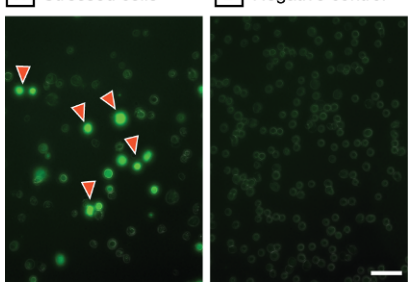

Figure 7: BA/F3-based cell sensors. Initial results with mouse pro B cells indicates a robust response to stressful conditions as shown in (A) with red arrowheads. Control cell populations have low baseline fluorescence as is seen in (B). Scale bar 40 μm.

3. Microfluidic perfusion for modulating the stem cell microenvironment

Sponsors
NIBIB
NSF Graduate Research Fellowship
Singapore A*STAR

Project Staff
Katarina Blagović , Laralynne Przybyla, Yi-Chin Toh

Overview

Stem cells are powerful biological models as they may offer insights to fundamental issues in biocomplexity, as well as developmental biology and disease pathogenesis. For these reasons, intense effort is being focused on characterizing and manipulating cellular microenvironment as it plays an important role in determining the biological state of embryonic stem cells (ESCs). However, conventional cell culture methods provide incomplete control over the cellular microenvironment, especially with respect to cell-secreted diffusible factors. Our approach is to use microfabricated culture systems to create a "neutral background" free of cell-secreted factors, and thus enable the study of defined media conditions for self-renewal and differentiation as a supplement to standard techniques. To this end, we have developed microfluidic devices that use perfusion to sweep away diffusible signals (cell-secreted factors), establishing a cleaner experimental system with more control over the soluble microenvironment.

Current Research

We have been focused recently on three aspects of this technology. First, because stem cells, and adherent mammalian cells in general, dynamically interact with their extracellular matrix (ECM) and culture substrate, controlling the ECM composition is critical to controlling cell state, and so we have been developing methods to integrate diverse materials for cell culture into our microfluidic devices. Second, we are investigating how microfluidic perfusion itself affects stem cell phenotype in self-renewal. Third, we are investigating how shear, even at the low levels used in perfusion, might affect stem cell phenotype.

Micropatterned polystyrene films for stem cell culture

The cell culture substrate itself is a potent modulator of cell fate. In particular, different substrates adsorb ECMs differently, which in turn affects cell attachment and function. Standard culture techniques typically utilize *tissue culture polystyrene* (TCPS), a treated polystyrene substrate that promotes cell attachment. Microfluidic devices, which are increasingly used for studying cell biology, typically use *glass* substrates, in part because of the compatibility of glass with standard microfabrication techniques, in particular polydimethylsiloxane (PDMS) bonding. However, glass substrates can alter both cell morphology and function for sensitive cells types such as embryonic stem cells (ESCs). We have developed a process that integrates micro-patterned polystyrene (MPPS) onto glass substrates, combining the cell-culture compatibility of polystyrene with the fabrication compatibility of glass.

We have developed a process that successfully combines the fabrication compatibility of glass with the culture compatibility of polystyrene (PS) substrates by using micro-patterned elastomeric

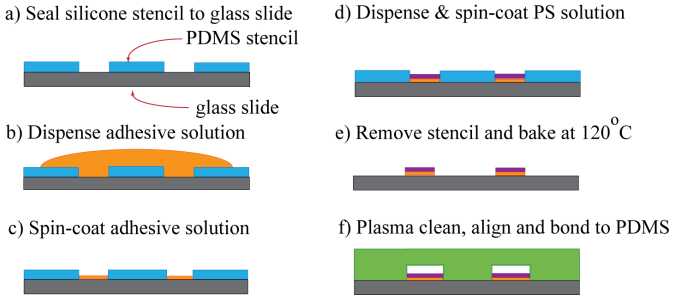

Figure 8. Process flow for patterning polystyrene on glass substrates using micropatterned PDMS stencils.

stencils to pattern dissolved polystyrene on glass substrates as indicated in Figure 8. We have integrated polystyrene patterns within previously developed two-layer microfluidic perfusion devices that incorporate pneumatically actuated valves. In this platform (Figure 9A) the polystyrene patterns serve a dual purpose – (1) as cell culture surfaces (Figure 9B) and (2) as valve seats for normally closed valves (Figure 9C). This illustrates a second advantage of the MPPS; since it does not bond to PDMS, we can use it to avoid irreversible bonding of the valve seat to the glass substrate. Additionally, such system allows for extraction of cells from individual chambers for further downstream off-chip analysis (qRT-PCR, FACS). Because adherent cells are sensitive to the topography and composition of the culture substrate, we characterized the MPPS surface properties by various techniques (Atomic Force Microscopy (AFM), X-ray photoelectron spectroscopy analysis (XPS), contact angle measurements, and a protein adsorption assay, using gelatin as a common matrix molecule for mouse ESC (mESC) cultures), and determined that they are comparable to TCPS.

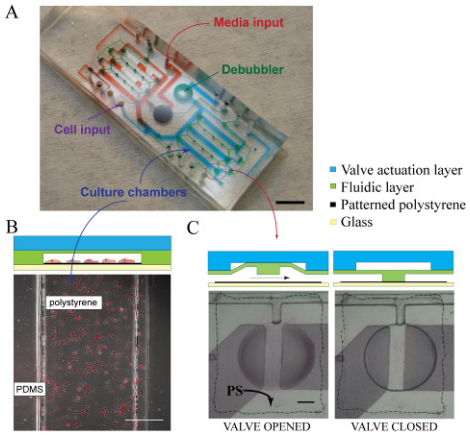

Figure 9. Applications of micro-patterned polystrene. (A) Image of a two-layer microfluidic device that incorporates cell culture chambers and normally closed valves. Scale bar 5 mm. (B) Top view of a MPPS culture chamber with NIH-3T3 mouse fibroblasts. Scale bar 150 μm. (C) Schematic of valve cross section (C, top). PS patterned valve seat prevents PDMS valve membrane from bonding (C, bottom). Scale bar 200μm.

Cell adhesion is a complex process, and a functional assays are ultimately needed to test any material system used as a culture substrate. We evaluated growth of mESC on various substrates (glass, TCPS, and MPPS). We found that proliferation and morphology of mESC on MPPS in static cultures was both qualitatively and quantitatively, as evaluated by image-based analysis of cell area, similar to that of TCPS and significantly improved over glass (Figure 10A-B).

To demonstrate the ability to integrate MPPS into microfluidic devices, we performed multi-day perfusion culture of mESC on our microfludic platform with integrated MPPS culture devices. Cells cultured on the MPPS surfaces showed improved morphologies over cells grown in glass chambers (Figure 10C).

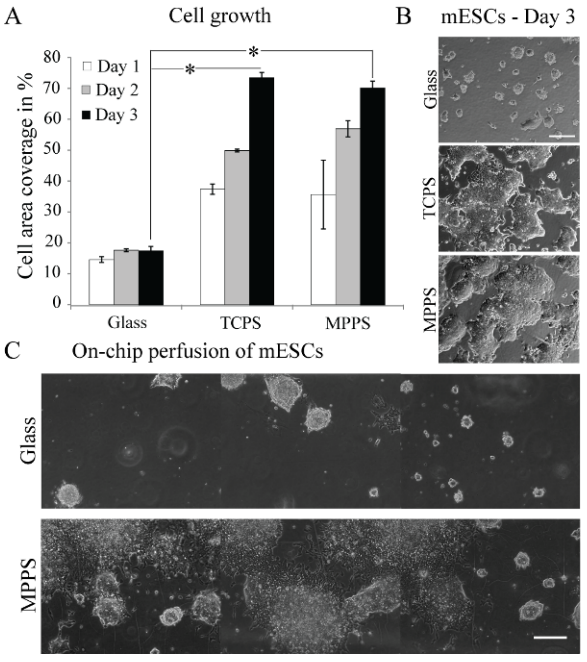

Figure 10. Growth of mESCs in static and perfused MPPS devices. (A) Cell proliferation and (B) morphology on MPPS was similar to that of TCPS and better than on glass. *Indicates statistical significance (Student's t-test, $p < 0.05$). (C) Multiday on-chip perfused culture of mESC. Phase images of mESC after 6 days of on-chip culture on glass and MPPS. mESCs on MPPS show better morphology and proliferation. Scale bars, 200 μm.

Modulation of diffusible signaling affects properties of mouse embryonic stem cells

Many factors contribute to the decision made by an embryonic stem cell to either remain as a stem cell or to differentiate into a specific cell type. These opposing options form the basis for the definition of an embryonic stem cell as a cell that can either maintain itself by self-renewal, or can differentiate into any cell type in the body, a property known as pluripotency. A major factor in this decision involves the external cues received by the cell, which include molecules secreted by surrounding cells. However, the ability to specifically control these external factors remains difficult. We are using microfluidic perfusion to sweep away diffusible molecules secreted by cells in order to create a neutral background. This allows for insight into the importance of secreted in maintaining stem cell self-renewal, and a determination of what default pathway a cell takes in the absence of secreted factors.

Upon growing mouse embryonic stem cells (mESCs) in defined, serum-free media conditions under perfusion, we have shown that perfusion in these conditions induces a change in cell phenotype. Using both quantitative RT-PCR and flow cytometry, we have seen lower levels of the stem cell markers Nanog and Oct4, and increased levels of the early differentiation marker Fgf5 in cells that were grown under perfusion for five days (Figure 11). Here, it is evident that the

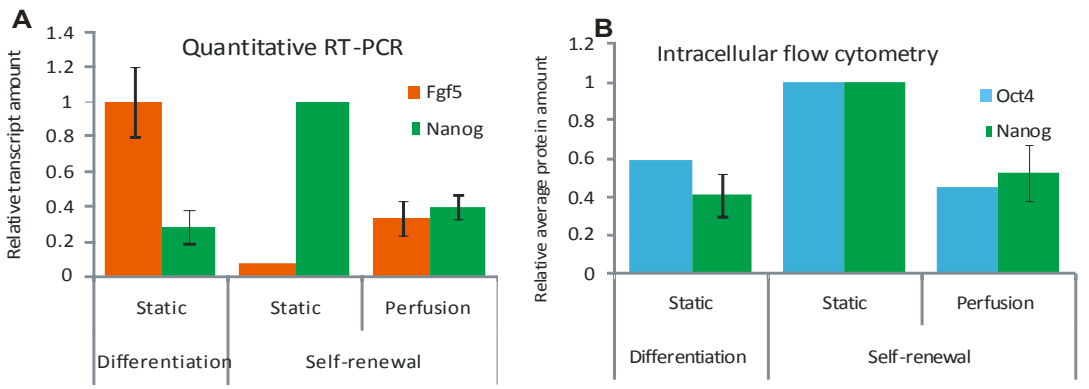

Figure 11. Comparison of self-renewal and differentiation factors between cells grown in static versus perfusion conditions. **(A)** Quantitative RT-PCR for expression of the early differentiation marker Fgf5 and the self-renewal marker Nanog in cells cultured in static versus perfused self-renewal conditions, showing increased differentiation under perfusion. Static differentiation results are included as controls. **(B)** Flow cytometric results for protein levels of the same conditions as in (A), this time comparing amounts of two self-renewal markers Oct4 and Nanog.

phenotype of cells grown under perfusion begins to resemble the phenotype of cells grown under differentiation conditions. This result implies that regulation of the embryonic stem cell microenvironment by removal of endogenously secreted factors potentially causes the cells to lose their pluripotent or self-renewing characteristics.

In order to further test this possibility, we performed downstream assays on cells that were grown under perfusion. After being exposed to perfusion for five days, cells were replated in static self-renewal growth conditions to assess their ability to continue to survive multiple passages. The perfusion cells were also replated in static differentiation conditions to monitor their morphology and assess their pluripotency. The results show that after undergoing perfusion, cells had decreased growth rates and decreased ability to self-renew (Figure 12).

These results all suggest a similar fate for mESCs grown under perfusion: that soluble secreted factors play an important role in maintaining mESCs as such, and once they are removed, mESCs begin a program of differentiation.

Microfluidic perfusion for shear stress studies

Stem cells are important for regenerative medicine and as *in vitro* models for drug testing and developmental studies. The stem cell microenvironment plays a vital role in determining stem cell fate; thus we need to understand and control these microenvironmental cues to fully exploit the potential of stem cells. While there has been substantial research on how soluble factors and extracellular matrices (ECM) affect stem cells, our understanding on stem cell responses to fluid shear stress is limited. Prior work has shown that by applying fluid shear stress corresponding to that in the developing heart, differentiation of stem cells into the cardiovascular lineage is significantly augmented. Although stem cell exposure to shear stress *in vivo* is predominantly limited to developing cardiovascular tissues, *in vitro* culture can subject bulk population of stem cells to shear stress, which can alter their phenotype. This is particularly true during the expansion of pluripotent stem cells for downstream applications in regenerative medicine, where bioreactors are typically used to culture the cells. Unintended alteration of stem cell phenotypes induced by fluid shear stress in bioreactors may jeapordize the application of the cultured stem cells for downstream applications. We aim to quantitatively investigate the effect of fluid shear stress on stem cells using a microfluidic perfusion system with multiple shear stress magnitudes.

To this end, we have designed and fabricated a 1x6 logarithmic flow rate PDMS microfluidic array device to simultaneously apply varying magnitudes of shear stress to stem cells (Figure 13). By

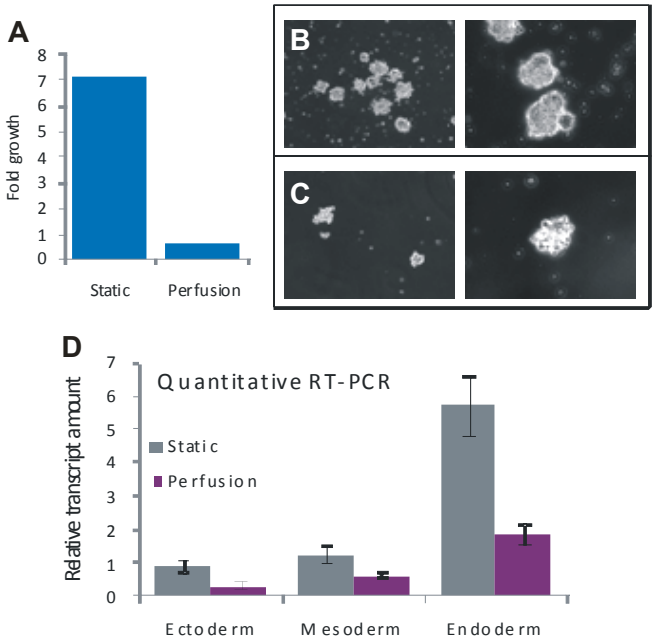

Figure 12. Downstream characteristics of mESCs are altered after undergoing perfusion. **(A)** The growth potential of cells was assessed after replating cells and growing for two passages in static self-renewal conditions. **(B-C)** The embryoid body prevalency and morphology was altered between cells that had been grown for five days in static (B) and cells that had undergone perfusion (C). **(D)** The embryoid body differentiation potential into all three germ layers was also decreased after cells had undergone perfusion.

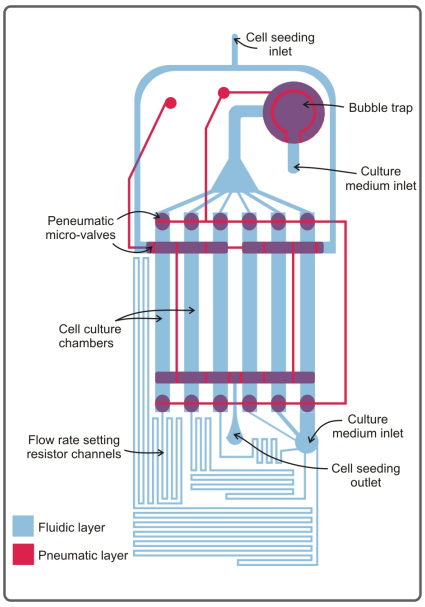

Figure 13. Schematic of the 1x6 logarithmic microfluidic perfusion array. The device consists of a fluidic layer with 6 cell culture chambers (blue), which are controlled with pneumatically actuated microvalves (red). Flow rate setting resistor channels determine the shear stress in each culture chamber.

specifying the dimensions of the flow rate-setting resistor channels, we are able to vary shear stress by a factor of 4 from channel to channel, enabling us to simultaneously study shear stress effects on stem cells over a range of 1024×. The device is optically transparent; hence it is amenable to imaging-based assays. The device is designed for reversible sealing so as to allow for off-chip cell analysis after shear stress application. For instance, we have designed a complementary vacuum-sealed PDMS chamber to harvest cell lysates from the individual perfusion chambers subjected to different shear stresses for subsequent analysis *e.g.,* quantitative real time PCR (qRT-PCR).

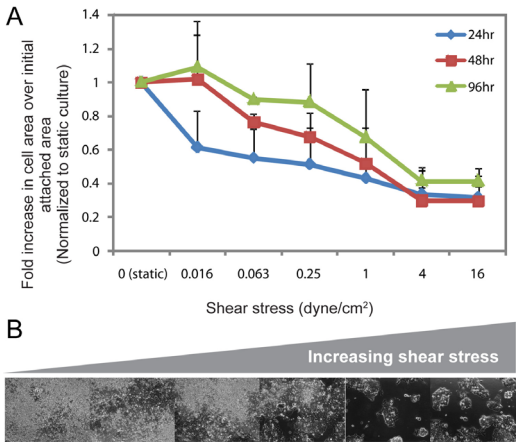

Figure 14. Effect of shear stress on proliferation of stem cells. **(A)** Proliferation as indicated by fold increase in stem cell colony area over the initial seeded cell area over a period of 72 hours. **(B)** Representative images from each perfusion chambers with different shear stress after 72 hours culture.

We used the logarithmic microfluidic perfusion arrays to investigate the effect of shear stress on stem cells under self-renewing conditions. This is to simulate flow conditions that may be experienced by stem cells when they are expanded in large-scale bioreactors. By using a closed-loop perfusion system driven by a peristaltic pump, we were able to achieve flow rates corresponding to shear stresses ranging from 0.016 to 16 dyne/cm^2. Image-based analysis of stem cell colony areas indicated that cell proliferation was negatively correlated to increasing shear stress magnitudes (Figure 14).

We also assessed the transcriptional expression of the stem cells using qRT-PCR after 72 hrs of shear stress application. We first investigated whether shear stress will affect the self-renewal of the stem cells by examining the expression of self-renewal markers, Nanog, Rex1 and Oct4 (Figure 15A). Although the cells were maintained in self-renewing medium, we observed a significant decrease in the expression of Nanog at shear stress higher than 1 dyne/cm^2. The

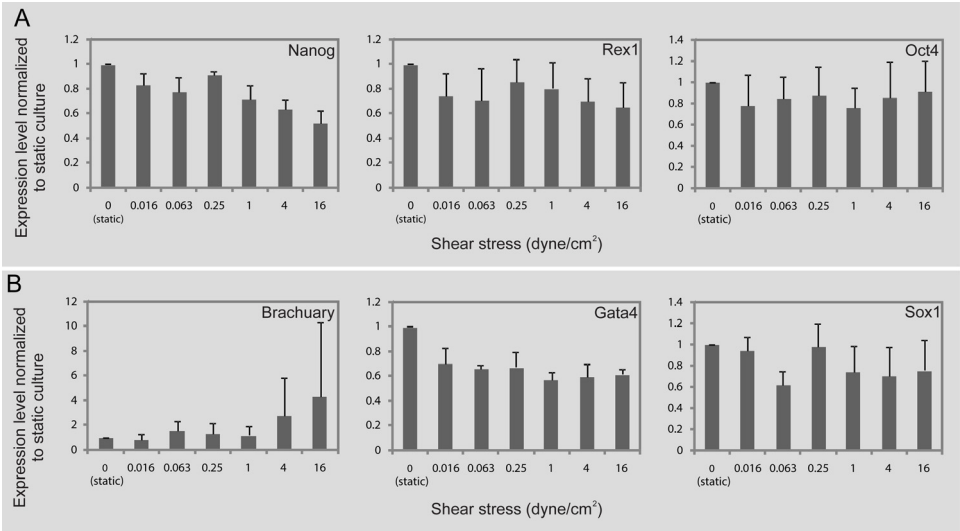

Figure 15. Transcriptional expression of stem cells exposed to different magnitudes of shear stress for 72 hours. (A) Self-renewal markers (B) Differentiation markers indicative of the 3 germ layers: mesoderm (Brachuary), endoderm (Gata4) and ectoderm (Sox1). Data are average ± SD of 3 independent devices.

expression of Oct4 and Rex1 were similar as compared to static controls. The decrease in Nanog, an important transcriptional regulator of self-renewability, prompted us to examine whether shear stress potentiates the differentiation of stem cells down a particular lineage. mRNA expression analysis of Brachuary (mesoderm marker), Gata4 (endoderm maker) and Sox1 (ectoderm marker) suggests that cultured stem cells under high shear stress (>4 dyne/cm^2) may predispose them to becoming mesodermal cells (Figure 15B).

We have demonstrated that our logarithmic microfluidic array is an effective platform to quantitatively investigate shear stress effects on stem cells over varying magnitudes. This improvement over current perfusion devices used for shear stress studies, where only one shear magnitude is applied at a time, will greatly facilitate our understanding of how fluid shear stress modulate stem cell fate.

4. Stem cell interactions and growth

Sponsors
NIH NCRR

Project Staff
Nikhil Mittal

Embryonic stem cells (ESCs) have the unique potential of being able to produce any cell type in the adult animal. While ESCs can differentiate to produce any type of cell, they can also divide to produce two daughter stem cells via self-renewal. Establishing proper culture techniques that permit self-renewal is a crucial step for maintaining stem cell cultures, as well as for expanding stem cell populations – a step that would likely precede any stem cell therapy. When expanding ESCs for therapeutic use, it will likely be important to do this via self-renewal, since the expansion potential of these cells decreases with increasing differentiation. For example, blood stem cells, which are currently the best characterized adult stem cells, can only be expanded ~20-fold *in vitro*. To study the requirements for cell growth, we have been investigating the effects of cell-cell interactions on the growth of mouse ESCs (mESCs). Cell-cell interactions consist of diffusible signaling and cell-cell contact (juxtacrine signaling), and are important in numerous biological processes such as tumor growth, stem cell differentiation, and stem cell self-renewal. We have previously demonstrated a new approach to modulating cell-cell signaling that modulates the local environment of a cluster of cells by placing different numbers of cells at desired locations on a substrate. Our method made use of the Bio Flip Chip (BFC), a microfabricated silicone chip containing hundreds-to-thousands of microwells, each sized to hold either a single cell or small numbers of cells.

We have used the BFC to study the effect of local density on the colony-forming efficiency (CFE) of mouse embryonic stem cells (mESCs). We found that the average single-cell colony-forming efficiency of mESCs increases with the number of cells in the initial cluster (Figure 16A), suggesting that cells within a cluster are communicating with each other. Next, we determined whether this effect is at least partly modulated by paracrine signaling. To do this, we plated single cells at different densities using the BFC, and found that the CFE did increase with density, suggesting that mESCs communicate via a diffusible survival factor (Figure 16B).

To validate the BFC-based approach, we have further investigated the system using traditional methods. We measured the effect of varying the plating density of cells on their growth and found that the growth rate of mESCs increases with the plating density for densities between 250 cm^{-2} and 10,000 cm^{-2}. This result validates the result obtained using BFC. We also checked that this effect is not merely due to varying attachment efficiencies, since this effect is prevalent from Day 1-2 of culture as well.

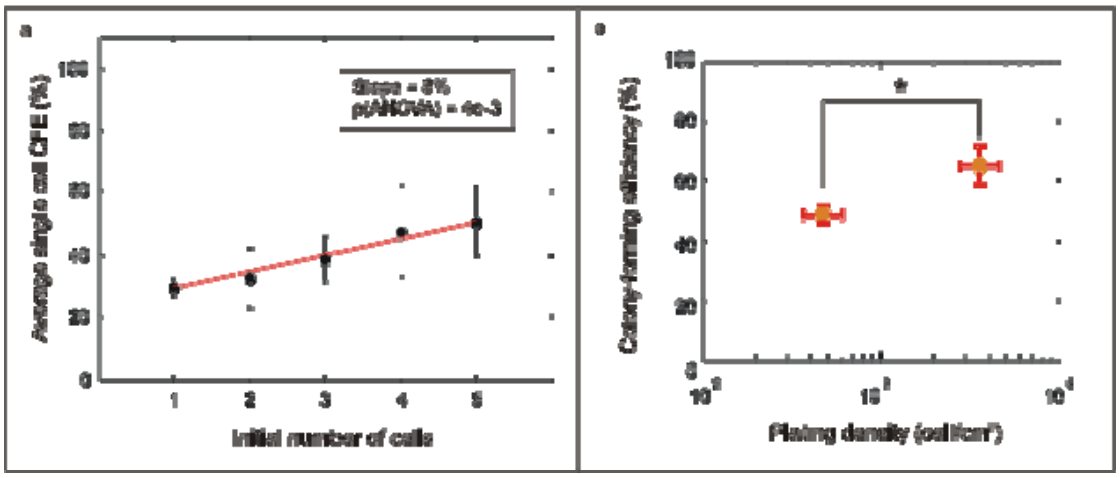

Figure 16: (a) The average colony-forming efficiency of a single cell in a cluster increases by ~6% for every cell added to a cluster (a). (b) The colony-forming efficiency increases by ~15% as the plating density increases from ~300 cm^{-2} to ~3000 cm^{-2}.

While density-dependent growth is often accepted as proof for the existence of an autocrine growth/survival factor, it is possible that the density-dependent growth increase could also result from the depletion of a growth inhibitor in the medium. To distinguish between the above two possibilities, we switched to performing our experiments in a defined medium (N2B27) to which LIF and BMP-4 are added to prevent the differentiation of mESCs. We collected conditioned medium (CM) from cells grown at 30,000 cm^{-2} and obtained the large molecule fraction (>3kDa) via dialysis. Then we added fresh low-MW components to control for nutrient depletion in the original CM. We observed that CM increased the growth rate of cells relative to control (Figure 17A). Next, we individually checked all the large (>3kDa) molecules in N2B27, as well as LIF and BMP-4, are not growth inhibitory for mESCs. Together, these results indicate that mESCs secrete a large-MW survival/growth factor.

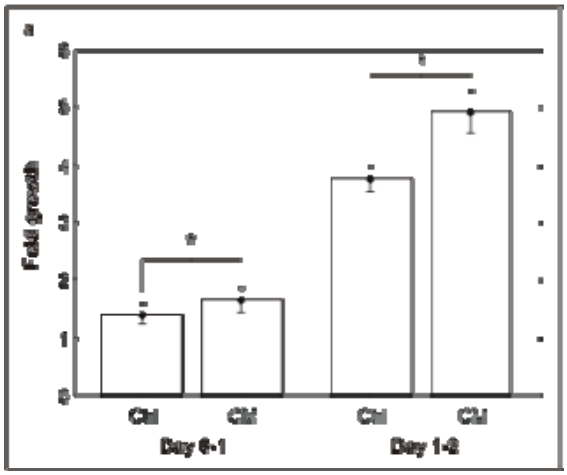

Figure 17: (a) Conditioned medium from cells grown at 10000-30000 cm^{-2} in N2B27 + LIF + BMP-4 improved the growth of mESCs. (b) Cyclophilin A improves the growth of mESCs in a dose-dependent manner.

5. Cell patterning-based approach for determination of autocrine spatial distribution and its impact on cell fate decision of murine embryonic stem cells

Sponsors
NIH NIBIB

Project Staff
Somponnat Sampattavanich

Overview

Heterogeneity during *in vitro* cultivation of embryonic stem cells (ESCs) is one major obstacle that postpones clinical usage of ESC for cell therapy. Recent studies demonstrated the role of autoregulatory signals in determining cell fates of ESCs. Our research aims to investigate the role of autocrine signaling on cell fate decision of ESCs and its potential contribution to the observed heterogeneity within ESC population. Prior techniques to examine autocrine signaling rely on bulk measurement of autocrine pathway activation using randomly plated cells. Such random cell positioning usually masks the effects of local autocrine ligand gradients, reducing chances to observe spatially varying cellular outcomes. In order to reconstruct the distribution of autocrine ligands based on the observed cell responses, we require a platform that can consistently maintain autocrine spatial distribution. Towards this goal, we have developed a cell patterning-based approach to microfabricate regular arrays of cells on the tissue culture substrate and to investigate changes in cell responses by systematically varying local and global autocrine ligand concentration. With uniform spacing between cell clusters, we postulate that the observed cell response will implicate the imposing autocrine ligand gradient. Having understood the contribution of autocrine signaling on ESC fate decision, we ultimately plan to develop techniques that can stably maintain pure undifferentiated population of ESCs as the unlimited cell supply for regenerative medicine.

Technology Background

To localize cells at precise locations on tissue culture substrates, we have chosen a stencil cell patterning technique. Unlike other cell patterning techniques that are based on substrate surface modification, stencil patterning allows cells to grow naturally out of the original patterning sites. A master mold initially microfabricated with SU8 photoresist on a silicon substrate is used to create thin silicone stencil membrane (Figure 18A). Each stencil membrane contains through holes positioned to match the desired location of cells on the tissue culture substrate. The stencil prevents cells from touching the substrate surface while allowing cells that can sink through the stencil holes to attach (Figure 18B).

Because the understanding of autocrine signaling in ESCs is limited, it is necessary that we first validate our developed platform using a better characterized autocrine system. A431 cells are epidermoid carcinoma cell which are known to express a large amount of epidermal growth factor receptors (EGFR) and secrete detectable amounts of transforming growth factor alpha (TGFα). Because TGFα can bind to EGFR and trigger its downstream signaling cascade, autocrine signaling in A431 cells had been postulated and validated by different investigators. Our results confirmed that cell proliferation of A431 cells was significantly enhanced by endogenous activation of EGFR signaling cascade (Figure 18C). Similar to prior studies, our study also demonstrated that the endogenous activation of EGFR diminishes when monoclonal antibodies against the TGFα/EGFR binding site were added to the culture media (Figure 18D). These findings substantiate A431 cells as a suitable model for validation of our platform

Having identified a model autocrine system, we attempted to determine the spatial distribution of autocrine signaling in A431 cells by constructing arrays of cell patches of various sizes and spacing. The goal of such patterning designs is to isolate the impact of global and local autocrine ligand concentrations. By comparing cell responses between different pattern configurations that can normalize either local or global autocrine ligand concentration, we can investigate the impact of autocrine spatial distribution on cell response and identify the critical spatial range at which cell responses transition between the different cell states.

Current Research

Using the developed platform, we have identified the range of colony spacing at which A431 cells transitioned from slow to fast growth in serum-free condition. Cells were patterned at two patch sizes, each with three different array spacings (Figure 18F). The patterning was designed such

that there will be pairs of patterned cell clusters with different patch sizes but still maintaining the same area fraction covered by cells over the same substrate area. Our results showed that the averaged cell proliferation per each cell cluster of the small and large patches were different for the intermediate (~30 radii) array spacing (Figure 18G). Because cells were cultivated in serum-free conditions, such change in cell growth must arise from the difference in the spatial distribution of autocrine signaling. To further substantiate our preliminary finding, we are currently working to observe more immediate cell responses such as phosphorylation of EGFR and ERK for different pattern configurations. A spatial map of the phosphorylation signals per cell will be generated and compared to the predicted autocrine ligand distribution. To improve throughput of the developed platform, we have recently established a new stencil design that will allow us to pattern multiple array configurations using only one device (Figure 18E). Cultivation between the different wells can be separated using reusable gaskets.

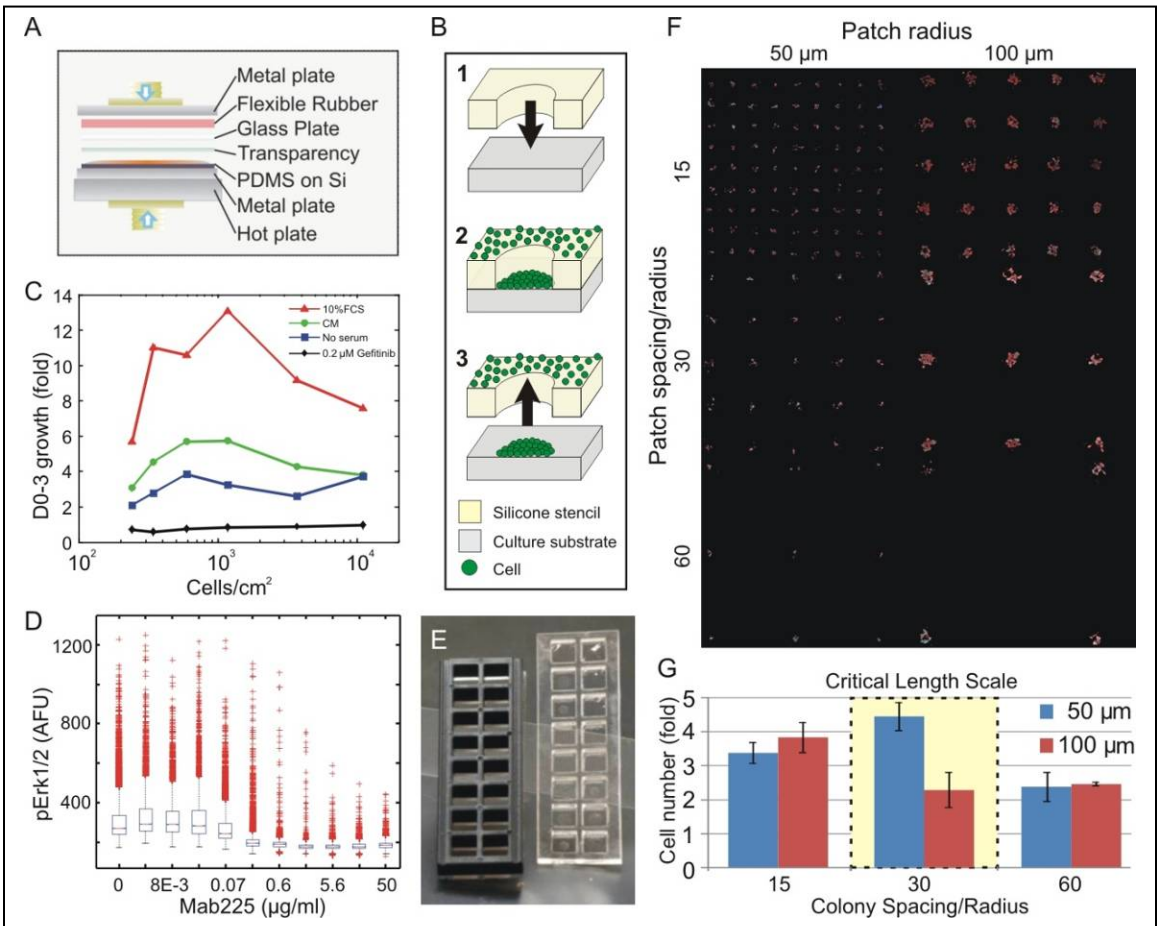

Figure 18: A) Stack of materials required to uniformly pressurize silicone to create stencil membrane. **B)** Stencil patterning procedure includes 1) apply stencil to culture substrate to obtain conformal contact, 2) load suspended cells and 3) peel off stencil after cell attachment. **C)** A431 cell growth when cultivated in different conditions at various initial plating cell densities. **D)** Phosphorylated ERK1/2 signal due to endogenous activation after 2 hours incubation with EGFR-blocking antibody (MAb225). **E)** New stencil design increases throughput of the platform. Black gasket is used to separate cultivation in different wells. **F)** Patterned A431 cells at varying patch sizes and spacing. **G)** Change in A431 growth after 24-hour cultivation in serum-free medium at various pattern configurations.

6. Microfluidic pairing and fusion for studying stem cell fusion and reprogramming

Sponsors
NIBIB

Project Staff
Melanie Hoehl

Overview:

Currently, several different methods have been used to reprogram somatic cells to an embryonic stem-cell-like state, including somatic cell nuclear transfer, forced expression of transcription factors, and cell fusion. Cell fusion is an appealing method by which to study reprogramming as the delivery of cells is easily visualized. However, conventional methods to fuse cells *en masse* do not control the pairing between cell populations, resulting in heterogeneous output populations that must be further purified.

Technology Background

We have developed a microfluidic system in which thousands of ESCs and somatic cells (SCs) are properly paired and immobilized, resulting in a high number of one-to-one fusions that can be clearly identified for further studies (Figure 19). The device consists of thousands of microscale cell traps in a millimeter-sized area. The traps consist of larger frontside and smaller backside capture cups made from a transparent biocompatible polymer. The key to pairing cells efficiently is to load them sequentially in a 3-step loading protocol enabling capture and pairing of two different cell types. The geometry of the capture comb precisely positions the two cells, and flow through the capture area keeps the cells in tight contact in preparation for fusion. With this approach we have obtained pairing efficiencies of ~70%.

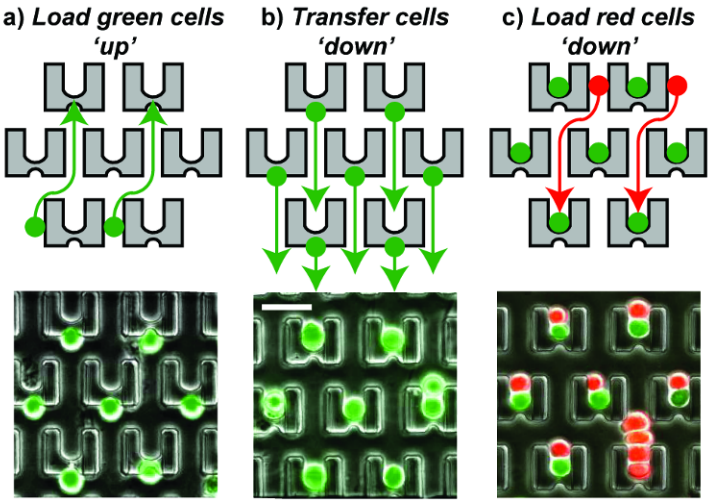

Figure 19. Three-step cell loading protocol. **(a)** Cells are first loaded "up" towards the smaller backside capture cup. **(b)** The direction of the flow is reversed, and the cells are transferred "down" into the larger frontside capture cup 2 rows below; scale bar, 50 μm. **(c)** The second cell type is loaded in from the top, and cells are captured in front of the first cell type.

The device is compatible with both chemical and electrical fusion, and, in agreement with the literature, we have obtained higher performance with electrofusion. When we compared fusion performance in our device to commercial approaches, we obtained significant improvements in overall performance for both PEG-mediated fusion and electrofusion. Specifically, we have measured fusion efficiencies of ~80% in our device using electrofusion, about 5× greater than that obtained in commercial systems. We are also able to remove fused cells from the device and culture them, demonstrating that the device creates viable fused cells (Figure 20a-b). Finally, by fusing mouse embryonic stem cells (mESCs) with mouse embryonic fibroblasts (mEFs, a somatic cell type), we have demonstrated the ability to reprogram the somatic cells to a

pluripotent state as evidenced by morphology, alkaline phosphatase staining (Figure 20c), and activation of an oct4-GFP reporter present in the somatic cell genome (Figure 20d). We are now studying the process of nuclear reprogramming of somatic cells by pairing and fusion of MEFs with pluripotent cells.

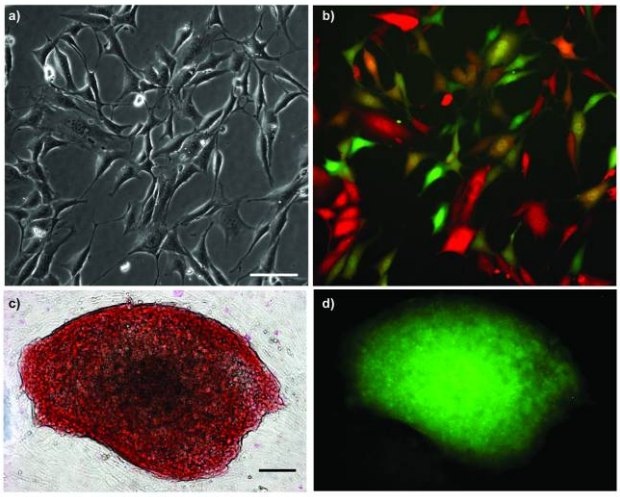

Figure 20. Functionality of fused cells. (a-b) Phase and fluorescent image of DSRed/EGFP fibroblasts at day 4 after fusion in the microfluidic device. scale bar, 100 μm. (c-d) Double-resistant hybrids between Hygromycin B-resistant mESCs and Puromycin-resistant mEFs after fusion in the microfluidic device, showing ESC-like morphology, positive alkaline phosphatase, staining, and reactivation of endogenous Oct4-GFP reporter; scale bar, 100 μm.

In addition we are developing a modified version of the device to study cell-cell interactions in immunology. Many immune responses are mediated by cell-cell interactions. For example, interactions with other cells stimulate the proliferation of T cells and lead to the activation of natural killer cells that kill pathogens and tumors. Similarly, the activation of antibody-producing B cells requires interactions with T cells. Studying these and other cell-cell interactions at a molecular scale is therefore crucial for understanding the dynamics and specificity of the immune response. Current methods to study cell-cell interaction involve plating labeled cells on a dish, searching for single conjugates and studying their interactions individually under a microscope. However, these methods suffer limitations of low time resolution, no directional control, and the ability to observe only a small number of cells---precluding the gathering of sufficient data for meaningful statistics. We expect that our modified cell-pairing device provides a number of new capabilities to overcome limitations of current methods, and will allow us to gain a deeper understanding about the time dependence, statistics and directionality of cell-cell interactions involved in the immune response.

7. Iso-Dielectric Separation for Continuous-Flow Cell Screening

Sponsors
NIBIB
Singapore-MIT Alliance

Project Staff
Michael Vahey, Salil Desai

Overview
Genetic or phenotypic screens require the ability to select a small fraction of targeted cells from a large, heterogeneous background. One of the greatest challenges in applied biology is to perform these screens in a way that possesses both high throughput and high purity. Our approach to this problem is to develop a new equilibrium method, called iso-dielectric separation (IDS), for sorting cells based upon electrically distinguishable phenotypes. Equilibrium methods sort cells according to their intrinsic properties, and thus do not require that any labels be developed and applied to the targeted cells. Furthermore, they have the potential to be both preparative and analytic, meaning that they are able to provide both separation as well as quantitative information about the population of cells. The IDS device developed in our lab exhibits all of these characteristics, and offers the additional advantage of operating under

continuous-flow. This enables high throughput, label-free, analytic and preparative separations capable of resolving multiple sub-populations of cells from heterogeneous backgrounds in a microfluidic format.

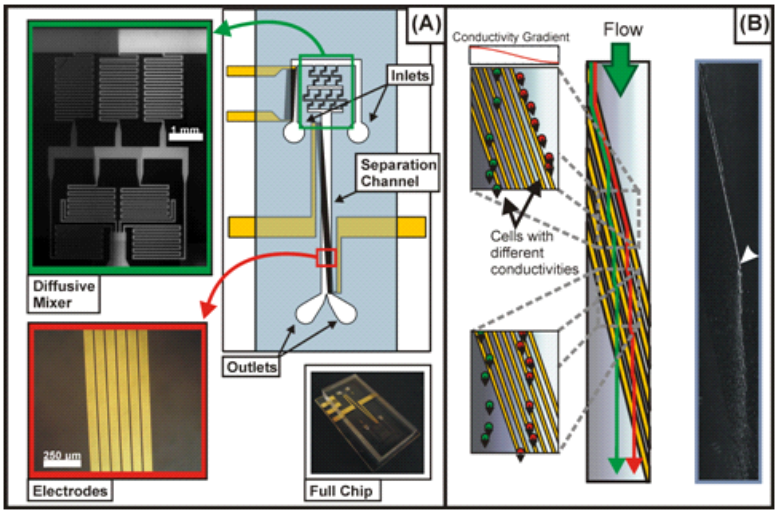

Figure 21: Concept and implementation of IDS. (A) Layout of the device, consisting of two inlets, a diffusive mixer to establish the electrical conductivity gradient, and a separation channel, along which diagonal pairs of electrodes are arranged. (B) Operation of the device: cells are carried by flow to electrodes across the channel diagonal. The DEP force resolves with hydrodynamic drag to direct the particle across the width of the channel, in the direction of decreasing conductivity and thus towards the iso-dielectric point (IDP). To the right is a fluorescence micrograph of polystyrene beads deflected by the electrodes prior to reaching their IDP (arrow).

Figure 21 presents an overview of the device concept and operation. A particle or cell in a spatially non-uniform electric field experiences a force proportional to its polarizability. Because the polarizability of a particle is a function of the electrical conductivity of that particle as well as that of the surrounding medium, a cell placed in a conductivity gradient spanning an appropriate range will be characterized by the point along this gradient where its polarizability vanishes. This corresponds to the matching of cell and medium electrical properties at a particular location, which we refer to as the iso-dielectric point (IDP). Using dielectrophoresis, it is possible to direct particles to their IDPs, enabling the separation of electrically distinguishable particles. Importantly, although the polarization of a cell generally depends on factors other than the electrical conductivity and permittivity (e.g. size and shape), by selecting cells based upon their IDPs, we are able to suppress sensitivity to these additional factors. Thus IDS offers the potential for conductivity-specific separations, even in the presence of large variability in size.

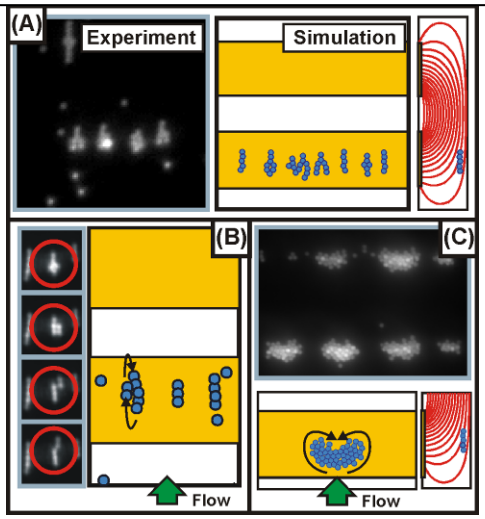

Figure 22: Emergent behavior in systems of interacting colloidal particles. (A) The coplanar electrode geometry under consideration as viewed from the side (right), along with static "wishbone" shaped particle clusters, observed experimentally and predicted by simulations. (B) Longer chains of polarized particles exhibit a treadmilling instability, in which particles from the weakly polarized back end of the chain periodically dissociate and flow forward, where they rejoin the chain. (B) Larger aggregates of particles form clusters which continually recirculate under hydrodynamic coupling.

Current Research

Particle-Particle Interactions

To better understand the performance of IDS and electrical separation methods in general, we are studying how particles subjected to electric and hydrodynamic fields couple to each other in microfluidic devices. This coupling can lead to substantial improvement or degradation in the performance of a separation (e.g. its throughput or purity) depending upon the particular mechanism by which separation is achieved. We have investigated the influence of particle

interactions on the fundamental behavior of colloidal suspensions (Figure 22) as well as their implications for devices designed to separate or concentrate colloidal particles.

Because the behavior of colloidal systems subjected to electric and hydrodynamic fields depends on the local concentration of particles, devices that modulate particle concentration over space and time are inherently non-linear and hysteretic, giving rise to a variety of dynamic behaviors under different operating conditions (Figure 22). To date, we have investigated how the specific mechanism by which separation is achieved affects this non-linearity to determine the purity of that separation. For example, we have found that changing the operating conditions of a separation over time can yield better performance in some cases compared to separations with static operating conditions. We have also performed case studies of two different electrical separation methods: IDS, and dielectrophoretic field-flow fractionation (DEP-FFF). In both methods, polarized particles coalesce into clusters at high particle concentrations and grow by entraining other particles. While for DEP-FFF, high purity separation requires low particle concentrations, we have found that IDS exhibits improved performance as the concentration of particles is increased.

More recently, we have developed a statistical model that captures important features of particle separation and concentration observed in experiments. This straightforward statistical model, combined with the direct numerical calculation of how particles interact electrically and hydrodynamically, should facilitate the design of novel separation devices that leverage particle interactions to achieve improved performance.

8. Cyborg moth flexible multi-electrode arrays

Sponsors
DARPA

Project Staff
Spencer Murray
Wei Mong Tsang

Overview

Significant interest exists in creating insect-based Micro-Air-Vehicles (i-MAVs) that would combine advantageous features of insects—small size, relatively large payload capacity, navigation ability—with the benefits of MEMS and electronics—sensing, actuation and information processing. The two basic components of an i-MAV are the telemetry system and stimulation system (Figure 23a). The telemetry system provides a communication link between the insect and the base station, while the stimulation system interfaces with the nervous system of the insect to bias the insect's flight path.

Our goal is to develop a flexible electrode array that provides multisite stimulation of the moth's abdominal nerve cord. These flexible multisite electrodes (FMEs) must be suitable for implantation into moth (*Manduca sexta*) pupae, and directly interface with the central nervous

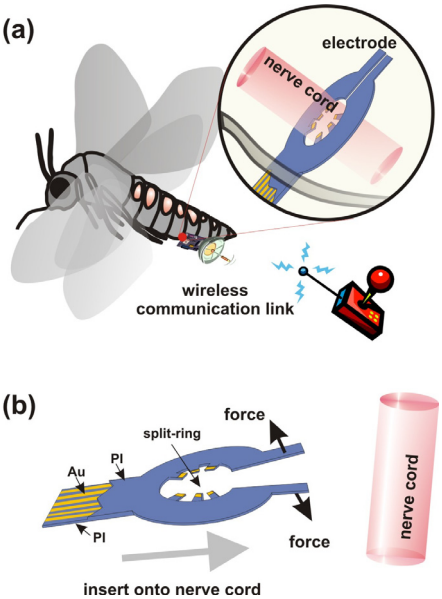

Figure 23. (a) Overview of i-MAVs, showing the communication link and the bioelectronic interface. **(b)** Schematic of the FME insertion process, showing how the split ring can be opened to fit around the nerve cord.

system (CNS) of the moth for flight control. This effort is a part of a larger joint project between the Massachusetts Institute of Technology, the University of Arizona and the University of Washington to develop the tools and technologies capable of guiding the flight of the self-powered moth.

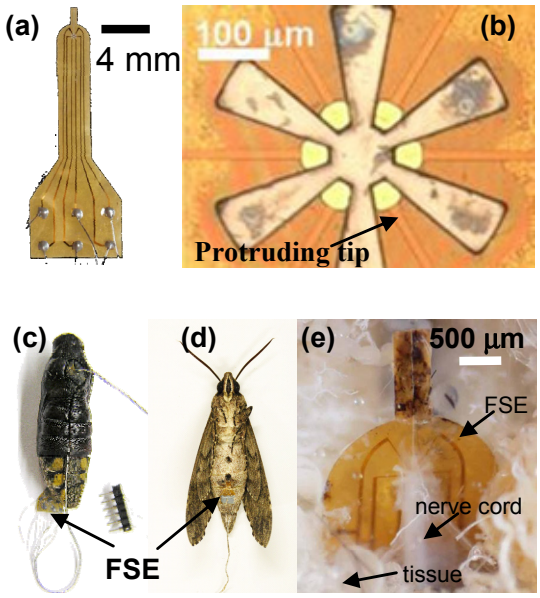

Figure 24. **(a)** Image of the FME with wire connection; **(b)** Close-up image of the FME at the split-ring region; **(c)** Image of a pupa with inserted FME; **(d)** Enclosed adult moth with FME inserted at the pupal stage; **(e)** Image of dissected adult moth showing the growth of connective tissue around the FME.

Technology Background

In this work, we have developed a flexible multisite electrode (FME) for insect flight control. The FME uses a set of electrodes arranged around a split ring to provide circumferential stimulation around an insect's nerve cord. The FME is made of two layers of polyimide (PI) with gold sandwiched in-between in a split-ring geometry. The stimulation sites are located at each end of protruding tips that are circularly distributed inside the split-ring structure. The split-ring design of the FME in conjunction with the flexibility of the PI allows us to split open the ring of the FME during insertion (Figure 23b). On the other hand, the protruding tips located inside the split-ring of the FME are still stiff enough to penetrate into the outer sheath of the nerve cord after insertion of the FME. Hence, the stimulation sites, which are located at the ends of the protruding tips, can directly stimulate the nerve cord

Current Research

Images of the fabricated FME are shown in Figure 24. We have been able to insert the electrode into pupae of Manduca sexta as early as 7 days before the adult moth emerges, and we are able to stimulate multi-directional graded abdominal motions in both pupae and adult moths. The direction of the abdominal movements depends on the particular pair of stimulation sites excited. The pupal implantation allows for tissue growth around the FME before the adult moth emerges, which enhances the attachment of the FME. Also, as compared to the adult moth, the body of the pupae is relatively immobile, easing the difficulty of insertion surgery. We have demonstrated that the FME is able to stimulate abdominal motion that can in turn cause ruddering to alter adult moth flight path (Figure 25).

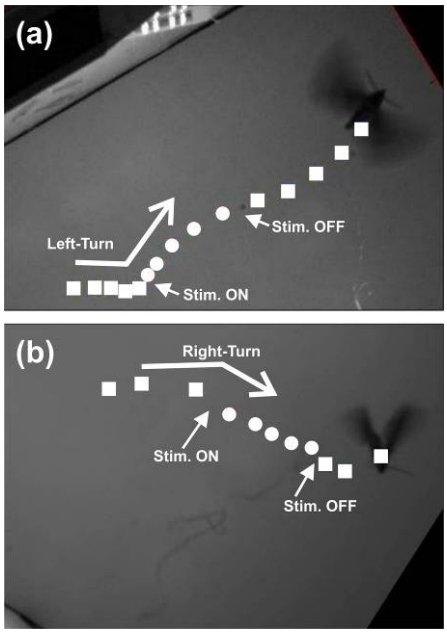

Figure 25. Images showing the loosely tethered moth that has been stimulated to perform **(a)** left and **(b)** right turns following the stimulation of the FSE. The flight path of the moth with and without FSE stimulation are tracked by solid circle (●) & solid square (■) dots, respectively.

Finally, we are developing a process for electroplating Au-CNT nanocomposite coatings on FMEs to reduce the stimulation voltage and enhance the charge injection capacity at the

interface between the electrode and nerve tissue of the moth. We have observed a decrease in impedance at the stimulating frequency of 100 Hz from 2.8 MΩ to 35 kΩ (Figure 26) and ~10-fold increase in the charge transfer after CNT coating (measurements in saline). Pupa implanted with FMEs coated with the Au-CNT nanocomposite are able to emerge into adult moths, and preliminary *in vivo* characterization shows that the FME is able to elicit strong abdomen flexions with stimulation voltage as low as 2.0 V, as compared to 5.0 V for 'bare' FMEs.

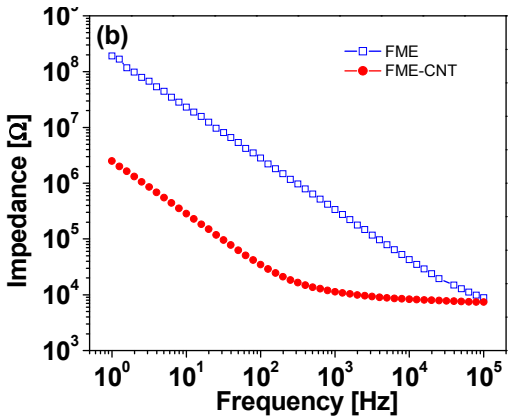

Figure 26. Impedance measurement results of bare and CNT-coated FMEs in saline showing a reduction of the impedance of the FME after CNT coating.

Publications

Journal Articles, Published

H.-H. Cui, J. Voldman, and K.-M. Lim, "Separation of particles by pulsed dielectrophoresis," *Lab on a Chip,* vol. 9, pp. 2306-12, 2009.

S. P. Desai, B. M. Taff, and J. Voldman, "A photopatternable silicone for biological microsystems " *Langmuir,* vol. 24, pp. 575-81, 2008.

S. P. Desai, M. D. Vahey, and J. Voldman, "Vesicle libraries - tools for dielectrophoresis metrology," *Langmuir,* vol. 25, pp. 3867-75, 2009.

S. P. Desai, D. M. Freeman, and J. Voldman, "Plastic masters - rigid templates for soft lithography," *Lab on a Chip,* vol. 9, pp. 1631-7, Jun 7 2009.

B. M. Taff, S. P. Desai, and J. Voldman, "Electroactive hydrodynamic weirs for microparticle manipulation and patterning," *Applied Physics Letters,* vol. 94, pp. 084102-3, 2009.

A. M. Skelley and J. Voldman, "An Active Bubble Trap and Debubbler for Microfluidic Systems," *Lab Chip,* vol. 8, pp. 1733-7, 2008.

A. M. Skelley, O. Kirak, H. Suh, R. Jaenisch, and J. Voldman, "Microfluidic Control of Cell Pairing and Fusion," *Nature Methods,* vol. 6, pp. 147-52, 2009.

M. D. Vahey and J. Voldman, "A new equilibrium method for continuous-flow cell sorting using dielectrophoresis," *Analytical Chemistry,* vol. 80, pp. 3135-43, 2008.

M. D. Vahey and J. Voldman, "Characterization of diverse cell and particle types using iso-dielectric separation," *Analytical Chemistry,* vol. 81, pp. 2446-55, 2009.

Books/Chapters in Books

J. R. Kovac, B. M. Taff, and J. Voldman, "Enabling technologies for image-based cell sorting," in *Microdevices in Biology and Medicine*, Y. Nahmias and S. Bhatia, Eds.: Artech House, 2009, pp. 129-48.

Meeting Papers, Presented

K. Blagovic, S. P. Desai, L. Y. Kim, and J. Voldman, "Patterned polystyrene substrates for integrated microfluidic culture devices," in *Biomedical Engineering Society Annual Meeting*, St. Louis, MI, 2008.

K. Blagovic, L. Y. Kim, and J. Voldman, "Microfluidic perfusion for modulating stem cell diffusible signaling in embryonic stem cell differentiation and self-renewal," in *6th International Society of Stem Cell Research Annual Meeting*, Philadelphia, PA, USA, 2008.

D. C. Daly, M. Bhardwaj, F. S. Lee, P. P. Mercier, D. D. Wentzloff, J. Voldman, and A. P. Chandrakasan, "Energy Efficient Pulsed-UWB Transceiver for Insect Flight Control," in *GOMACTech*, Las Vegas, NV, 2008.

S. P. Desai and J. Voldman, "Measuring the Impact of Dielectrophoresis on Cell Physiology using a High-Content Screening Platform," in *Biomedical Engineering Society Annual Meeting*, St. Louis, MI, 2008.

J. R. Kovac and J. Voldman, "Microscopy-based Sorting of Adherent Cells Using Photopolymerization-activated Cell Sorting " in *Biomedical Engineering Society Annual Meeting*, St. Louis, MI, 2008.

N. Mittal and J. Voldman, "Exploring cell-cell communication in mouse embryonic stem culture using bio flip chips," in *6th International Society of Stem Cell Research Annual Meeting*, Philadelphia, PA, USA, 2008.

S. Sampattavanich and J. Voldman, "Examining the effective autocrine length scale using stencil cell patterning," in *Biomedical Engineering Society Annual Meeting*, St. Louis, MI, 2008.

S. Sampattavanich and J. Voldman, "Matrix-independent colony patterning to study the influence of colony-colony interactions on stem cell fate decision in murine embryonic stem cells," in *6th International Society of Stem Cell Research Annual Meeting*, Philadelphia, PA, USA, 2008.

S. Sampattavanich, B. M. Taff, and J. Voldman, "Organizing complex multicellular constructs using stencil-delineated electroactive patterning (S-DEP)," in *Biomedical Engineering Society Annual Meeting*, St. Louis, MI, 2008.

A. M. Skelley, O. Kirak, R. Jaenisch, and J. Voldman, "A Massively Parallel Microfluidic System for Studying Fusion-based Reprogramming," in *6th International Society of Stem Cell Research Annual Meeting*, Philadelphia, PA, USA, 2008.

N. Tandon, A. Marsano, C. Cannizzaro, J. Voldman, and G. Vunjak-Novakovic, "Design of electrical stimulation bioreactors for cardiac tissue engineering," in *30th Annual International Conference of the IEEE-EMBS*, Vancouver, CA, 2008.

M. D. Vahey and J. Voldman, "High-throughput characterization of electrical phenotype using iso-dielectric separation," in *Biomedical Engineering Society Annual Meeting*, St. Louis, MI, 2008.

M. D. Vahey and J. Voldman, "Sorting concentrated cell suspensions: particle interactions and microfluidic separations," in *Biomedical Engineering Society Annual Meeting*, St. Louis, MI, 2008.

Meeting Papers, Published

K. Blagovic, L. Y. Kim, A. M. Skelley, and J. Voldman, "Microfluidic control of stem cell diffusible signaling," in *Micro Total Analysis Systems '08*, San Diego, CA, USA, 2008, pp. 677-679.

H.-H. Cui, K.-M. Lim, and J. Voldman, "Experiment and modeling of pillar array micro-traps with negative dielectrophoresis," in *Micro Total Analysis Systems '08*, San Diego, CA, USA, 2008, pp. 1012-14.

S. P. Desai and J. Voldman, "Measuring the impact of dielectrophoresis on cell physiology using a high-content screening platform," in *Micro Total Analysis Systems '08*, San Diego, CA, USA, 2008, pp. 1308-10.

J. R. Kovac and J. Voldman, "Image-based cell sorting using optofluidics," in *2008 IEEE/LEOS Summer Topical Meeting on Optofluidics*, Acapulco, Mexico, 2008.

T. D. Robinson, B.-H. Ooi, B. M. Taff, K. E. Willcox, and J. Voldman, "Surrogate-Based Optimization of a Microfluidic Weir Structure for Single-Cell Manipulation," in *12th AIAA/ISSMO Multidisciplinary Analysis and Optimization Conference* Victoria, British Columbia, Canada, 2008.

S. Sampattavanich, B. M. Taff, S. P. Desai, and J. Voldman, "Organizing complex multicellular constructs using stencil-delineated electroactive patterning (S-DEP)," in *Micro Total Analysis Systems '08*, San Diego, CA, USA, 2008, pp. 567-69.

A. M. Skelley and J. Voldman, "An active, integrated bubble trap and debubbler for microfluidic applications," in *Micro Total Analysis Systems '08*, San Diego, CA, USA, 2008, pp. 1360-62.

W. M. Tsang, Z. Aldworth, A. Stone, A. Permar, R. Levine, J. G. Hildebrand, T. Daniel, A. I. Akinwande, and J. Voldman, "Insect flight control by neural stimulation of pupae-implanted flexible multisite electrodes," in *Micro Total Analysis Systems '08*, San Diego, CA, USA, 2008, pp. 1922-24.

M. D. Vahey and J. Voldman, "Sorting concentrated suspensions: particle interactions, emergent behavior, and implications for microfluidic separations," in *Micro Total Analysis Systems '08*, San Diego, CA, USA, 2008, pp. 1474-76.

M. D. Vahey and J. Voldman, "High-throughput cell and particle characterization using isodielectric separation," in *Micro Total Analysis Systems '08*, San Diego, CA, USA, 2008, pp. 1187-89.

D. C. Daly, P. P. Mercier, M. Bhardwaj, A. L. Stone, J. Voldman, R. Levine, J. G. Hildebrand, and A. P. Chandrakasan, "A Pulsed UWB Receiver SoC for Insect Motion Control," in *ISSCC*, San Francisco, 2009.

Theses

B. M. Taff, *Microsystems Platforms for Array-based Single-cell Biological Assays*, Ph. D. diss., Department of Electrical Engineering and Computer Science, 2008.

S. P. Desai, *Building Integrated Cell-based Microsystems: Fabrication Methodologies, Metrology Tools, and Impact on Cellular Physiology*, Ph.D. thesis, Department of Electrical Engineering and Computer Science, 2009.